Journal of Alzheimer's Disease 61 (2018) 673–688
DOI 10.3233/JAD-170393
IOS Press

Increased Foxo3a Nuclear Translocation and Activity is an Early Neuronal Response to βγ-Secretase-Mediated Processing of the Amyloid-β Protein Precursor: Utility of an AβPP-GAL4 Reporter Assay

Bernard M. Law[a], Amy L. Guest[a], Matthew W. J. Pullen[a], Michael S. Perkinton[b] and Robert J. Williams[a,*]
[a]*Department of Biology and Biochemistry, University of Bath, Bath, UK*
[b]*IMED Neuroscience, AstraZeneca, Granta Park, Cambridge, UK*

Handling Associate Editor: Mitchell Lai

Accepted 26 September 2017

Abstract. Sequential cleavage of the amyloid-β protein precursor (AβPP) by BACE1 (β-secretase) followed by the γ-secretase complex, is strongly implicated in Alzheimer's disease (AD) but the initial cellular responses to these cleavage events are not fully defined. β-secretase-mediated AβPP processing yields an extracellular domain (sAβPPβ) and a C-terminal fragment of AβPP of 99 amino acids (C99). Subsequent cleavage by γ-secretase produces amyloid-β (Aβ) and an AβPP intracellular domain (AICD). A cellular screen based on the generation of AICD from an AβPP-Gal4 fusion protein was adapted by introducing familial AD (FAD) mutations into the AβPP sequence and linking the assay to Gal4-UAS driven luciferase and GFP expression, to identify responses immediately downstream of AβPP processing in neurons with a focus on the transcription factor Foxo3a which has been implicated in neurodegeneration. The K670N/M671L, E682K, E693G, and V717I FAD mutations and the A673T protective mutation, were introduced into the AβPP sequence by site directed mutagenesis. When expressed in mouse cortical neurons, AβPP-Gal4-UAS driven luciferase and GFP expression was substantially reduced by γ-secretase inhibitors, lowered by β-secretase inhibitors, and enhanced by α-secretase inhibitors suggesting that AICD is a product of the βγ-secretase pathway. AβPP-Gal4-UAS driven GFP expression was exploited to identify individual neurons undergoing amyloidogenic AβPP processing, revealing increased nuclear localization of Foxo3a and enhanced Foxo3a-mediated transcription downstream of AICD production. Foxo3a translocation was not driven by AICD directly but correlated with reduced Akt phosphorylation. Collectively this suggests that βγ-secretase-mediated AβPP processing couples to Foxo3a which could be an early neuronal signaling response in AD.

Keywords: AICD, Akt, Alzheimer's disease, amyloid-β protein precursor, apoptosis, β-secretase, Forkhead transcription factor, FOXO3 protein, γ-secretase, neurodegeneration

INTRODUCTION

Despite ongoing debate about the validity of the amyloid cascade hypothesis, it is still the best explanation for the underlying triggering events in both

*Correspondence to: Robert J. Williams, Department of Biology and Biochemistry, University of Bath, Claverton Down, Bath, BA2 7AY, UK. Tel.: +44 0 1225 386553; E-mail: r.j.williams@bath.ac.uk.

sporadic and familial Alzheimer's disease (FAD), and it remains a key therapeutic target area for early intervention and risk reduction [1, 2]. Multiple cell types undeniably play a role in the development of amyloid-β (Aβ) pathology [3], but aberrant processing and metabolism of the amyloid-β protein precursor (AβPP) in neurons is still the most plausible disease-initiating event.

Soluble oligomeric forms of Aβ peptide, generated from AβPP, play a central role in AD pathogenesis and through actions at synapses affect excitability, plasticity, and neuronal viability triggering secondary pathologies such as development of dystrophic neurites and inflammation. Aβ is produced from sequential cleavage of AβPP, first by BACE1 (β-secretase) [4–7] to yield a large secreted extracellular domain (sAβPPβ) and an intracellular C-terminal fragment of AβPP of 99 amino acid (C99), followed by cleavage of C99 by γ-secretase [8, 9] to produce Aβ and an AβPP intracellular domain (AICD), which can potentially form a transcriptionally active complex with Fe65 and Tip60 [10]. Alternatively, AβPP can be cleaved by α-secretase to release neurotrophic sAβPPα and an intracellular C-terminal fragment of AβPP of 83 amino acids (C83) followed by cleavage of C83 by γ-secretase to yield a p3 fragment and an AICD [11]. To facilitate identification of inhibitors and modulators of these pathways and to investigate the pathophysiological regulation of AβPP metabolism, we adapted a gene reporter assay based on the cleavage of an AβPP-GAL4 fusion protein similar in principle to that used in HeLa [10–12], HEK293 [13], and SH-SY5Y cells [14]. To ensure that AβPP processing was assessed in a physiologically meaningful context, particularly to include the complexity of the post synaptic density, we employed the assay in mouse primary cortical neurons and demonstrated that excitatory synaptic transmission exerts a fine activity-dependent control over AβPP processing [15, 16]. This, therefore, potentially represents a powerful model system to investigate environmental and genetic influences on AβPP processing in a neuronal context enabling assessment of resulting changes in synaptic responsiveness and neuronal viability. We used this approach to test the hypothesis that amyloidogenic processing of AβPP couples to the pro-apoptotic transcription factor Foxo3a which has been reported to mediate AβPP-induced cell death through an AICD dependent pathway [17].

Lifelong overexpression of AβPP can cause AD, and numerous missense mutations in AβPP have been identified which lead to FAD [2]. Not all mutations in AβPP increase β-secretase processing and Aβ production *per se* but may instead result in elevated levels of C-terminally extended Aβ or increased ratios of long to short forms of the peptide such as the V717L (London) mutation [18]. Mutations in AβPP within the Aβ sequence itself, such as the E693G (Arctic), typically increase the self- aggregation properties of the peptide and enhances protofibril formation [19] which could accelerate neurotoxicity. There are some mutations in AβPP that do alter the levels of Aβ most notably the K670N/M671L (Swedish) mutation immediately adjacent to the β-secretase cleavage site [20, 21] and the E682K (Leuven) mutation which shifts processing toward the β-site increasing total Aβ production [22]. Significantly, the A673T mutation reduces β-secretase cleavage of AβPP, lowering Aβ production, and conferring protection against AD [23]. These mutations were introduced into the AβPP-GAL4 construct to assess their impact on the processing of AβPP, the sensitivity of processing to α-, β-, and γ-secretase inhibition and to identify early responses to amyloidogenic AβPP processing in neurons. For this, we focused primarily on potential downstream effects on Foxo3a-activity [24] which have previously been implicated in the development of protein pathology in neurodegenerative disease [25–27], likely through control of apoptosis and autophagy [28]. When used in primary cortical neurons, the AβPP-GAL4 assay preferentially reported βγ-secretase processing, was sensitive to mutations which influence β-secretase activity and revealed increased nuclear localization of Foxo3a and upregulation of Foxo3a activity as early events lying downstream of amyloidogenic AβPP processing. The recruitment of Foxo3a correlated with subtle reductions in the levels of Akt phosphorylation. Overexpressing GFP tagged AICD within the cytoplasm did not drive Foxo3a translocation to the nucleus but did enhance transcription. Collectively this suggests that βγ-secretase-mediated AβPP processing increases Foxo3a translocation and transcriptional activity which could be an early neuronal signaling response in AD.

MATERIALS AND METHODS

Antibodies and compounds

Mouse anti-GFP antibody (1 : 2000) was purchased from Abcam; Rabbit anti-FOXO3a (75D8) antibody (1 : 300) and rabbit anti-pAkt^{S473} antibody

(1 : 500) were obtained from Cell Signaling Technology; Rabbit anti-Amyloid Precursor Protein, C-Terminal amino acid 676-695 (1 : 2000; A8717) was purchased from Sigma. Goat anti-rabbit antibody Alexa Fluor 546 (1 : 600) and goat anti-mouse antibody Alexa Fluor 488 (1 : 2000) were purchased from Invitrogen. 4',6-Diamidino-2-Phenylindole, Dihydrochloride (DAPI; 1 mg/ml) from ThermoFisher Scientific. TAPI-1, Batimastat and β-secretase inhibitor IV (β-IV) were purchased from Merck Millipore, DAPT and BMS299897 were from Tocris Bioscience, AZD3839 from Selleckchem and GI 254023X from Sigma Aldrich. All secretase inhibitors were reconstituted in dimethylsulphoxide (DMSO) at stock solutions of 1-10 mM as recommended by the manufacturer.

Plasmids and site-directed mutagenesis

The AβPP-GAL4 plasmid containing the cDNA encoding full length AβPP695 and the yeast transcription factor GAL4 at the C-terminus of AβPP and the plasmid for expression of the Fe65 adaptor protein were as previously described [15]. The UAS-GFP plasmid, with the upstream activating sequence (UAS) lying immediately upstream of the GFP gene [29], was kindly provided by Dr. Zhiyang Gong (National University of Singapore, Singapore). pEGFP-n1-AICD was a gift from Zita Balklava and Thomas Wassmer [30] and was supplied by Addgene (plasmid # 69925). The Foxo3a response element (FRE) luciferase plasmid (FRE-Luc), containing three repeats of the insulin response element [31] upstream of the luciferase gene, was generated as previously described [32]. The pFR-Luc reporter plasmid, containing the firefly (*Photinus pyralis*) luciferase gene under the control of a synthetic promoter consisting of five tandem repeats of the yeast GAL4 activation sequence upstream of a minimal TATA box, and TK-Renilla, a phRL-thymidine kinase (TK) vector containing the sea pansy (*Renilla reniformis*) luciferase gene under the control of the HSV (herpes simplex virus)-TK promoter, were purchased from Promega. The generation of AβPP-GAL4 mutants was performed by site-directed mutagenesis using Pfu Ultra II Hotstart PCR Master Mix (Agilent Technologies). Mutated plasmids were cloned using the One Shot TOP10 Chemically Competent *E. coli* (Invitrogen) and subsequently obtained using a plasmid extraction kit (Qiagen). The correct incorporation of each mutation into the plasmid was confirmed by DNA sequencing.

Primary neuronal culture

Primary cortical neurons were prepared from CD1 mouse embryos in accordance with UK Home Office Guidelines as stated in the Animals (Scientific Procedures) Act 1986 using Schedule 1 procedures approved by the University of Bath Animal Welfare and Ethical Review Body. Primary neurons were prepared essentially as described previously [33]. Cortices were dissected from 15-day-old CD1 mouse embryos, and were mechanically dissociated in PBS supplemented with 33 mM glucose, using a fire-polished glass Pasteur pipette. Cells were plated into either 12- or 24-well Nunc tissue culture plates, previously coated with 20 μg/ml poly-D-lysine (Sigma). Neurons were cultured in Neurobasal medium (phenol red free) supplemented with 2 mM glutamine, 100 μg/ml penicillin, 60 μg/ml streptomycin, and B27 (all from Invitrogen), and incubated at 37°C, in high humidity with 5% CO_2. Under these growth conditions at 5–11 days *in vitro* (DIV) cells had a well-developed neuritic network and were 99% β-tubulin III positive and <1% GFAP positive.

Dual-Glo luciferase assay

0.5 μg of each of the required plasmid construct, including AβPP-GAL4, Fe65, pFR-Luc, TK-Renilla, FRE-Luc, and pEGFP-n1-AICD were first transfected into primary cortical neurons in 24-well tissue culture plates at 5–8 DIV using lipofectamine 2000 (0.5 μl/well) (Invitrogen) as recommended in the manufacturer's protocol. Mixtures of lipid and DNA were prepared in Opti-MEM I reduced serum medium (Invitrogen). The contents were mixed and incubated at room temperature for 25 min and the resulting transfection mixtures applied to the neurons dropwise directly into the growth medium (100 μl/well). The neurons were then returned to the incubator. Treatment of neurons with secretase inhibitors was typically performed 30 min prior to transfection. Neurons were processed for luciferase expression 24 h post-transfection. Neuronal lysis was achieved by incubation in Glo lysis buffer (Promega) (50 μl/well) with gentle agitation for 15 min. Lysates were transferred to a white 96-well microplate (Greiner Bio One) and then treated with Dual-Glo luciferase reagent (Promega) (50 μl/well). The subsequent quantification of the firefly luciferase reporter gene activity was performed using a Promega Glomax Multi Detection System. To control for the difference in transfection efficiency and neuronal

viability across wells, the firefly luciferase reporter activity was normalized to the Renilla luciferase activity to obtain the normalized luciferase signal. For the purposes of statistical analysis an individual transfected well of neurons was assigned $n = 1$ and experiments were typically repeated on cultures prepared from 2–3 maternal mice.

Immunofluorescence, confocal microscopy, and image acquisition

For microscopic analysis, cortical neurons were grown on 13 mm glass coverslips (Thermo Scientific) pre-coated with 20 μg/ml poly-D-lysine and placed in 12-well tissue culture plates. 1 μg of the required plasmid constructs, including AβPP-GAL4 and UAS-GFP, and 4 μg of pEGFP-n1-AICD were transfected into the neurons at 5–8 DIV, using lipofectamine 2000 (1 μl/well) (Invitrogen) as described above and transfection mixtures were added at 150 μl/well. Treatment of neurons with secretase inhibitors was performed as described in the Results section.

For direct live cell imaging and morphological assessment of GFP expressing neurons images were captured on an AMG EVOS LED fluorescence microscope 24–96 h after transfection. For immunofluorescence, cells were washed in prewarmed Neurobasal medium and then fixed in 4% paraformaldehyde in PBS at room temperature for 20 min. Neurons were permeabilized in PBS containing 0.5% Triton-X100 (Sigma) for 10 min, and were then incubated in a blocking buffer comprising PBS containing 3% bovine serum albumin (BSA) (Sigma) and 0.1% Triton-X100 for 30 min. This was followed by an overnight incubation of the cells in the appropriate primary antibodies added to an antibody buffer (PBS containing 1% BSA and 0.1% Triton X-100) at 4°C. The cells were then incubated in the appropriate secondary antibodies diluted in the antibody buffer for 1 h at room temperature. Neurons were counterstained for nuclei with DAPI (300 nM) for 20 min. Multi-channel fluorescence images were captured using either a 40X or 63X oil objective fitted to a Zeiss META LSM510 confocal microscope, using Zeiss LSM image examiner software (Carl Zeiss, Thornwood, NY). Multi-channel image overlays were obtained using ImageJ software (NIH, USA). Alexa fluorochromes were excited by the argon (488 nm) and helium/neon (543 nm and 633 nm) lasers at fixed exposure time and the emitted fluorescence was detected using the multi-track function and a combination of filters (550–625) and band pass filters (BP 420–480 and BP 505–530). All images were obtained using the Plan-Apochromat 63 × 1.4 NA oil objective. Z stack images were taken at 1 μm intervals.

Data analysis and statistics

AβPP-GAL4 driven luciferase expression data was analyzed by two-way ANOVA with a Bonferroni post hoc test (raw data), or by one-way ANOVA with a Dunnett's *post hoc* test (% comparisons to control). FRE-luc expression data and GFP cell expression data were analyzed by a two-tailed Student's *t* test. All analysis was undertaken using GraphPad Version 5 (La Jolla, CA) software and differences between experimental treatments were considered to be statistically significant when $p < 0.05$.

RESULTS

AβPP-GAL4 driven luciferase expression reports βγ-secretase-mediated AβPP processing in neurons

In order to assess the impact of AβPP mutations on secretase-mediated processing in primary cortical neurons, the K670N/M671L, E682K, E693G, and V717I FAD mutations, and the A673T protective mutation were introduced into the AβPP-GAL4 sequence by site directed mutagenesis. The luciferase reporter assay works on the principle that γ-secretase cleavage releases an AICD-GAL4 which then drives luciferase expression via the UAS. To establish the γ-secretase sensitivity of the different constructs two structurally distinct γ-secretase inhibitors, DAPT and BMS299897 were tested (Fig. 1A, B and Supplementary Fig. 1). Cortical neurons were treated with DAPT (10 μM) or BMS299897 (10 μM) 30 min prior to transfection with the respective AβPP-GAL4 and luciferase construct, together with TK-Renilla as an internal control and luciferase expression measured 24 h later. DAPT treatment resulted in a 57% reduction in luciferase expression as a result of wild type AβPP-GAL4 processing. The level of inhibition with DAPT was significantly greater for the processing of FAD AβPP-GAL4 mutants: 82% for K670N/M671L; 74% for E683K; 77% for E693G; 80% for V717I (Fig. 1A, B). In contrast, the protective A673T mutant showed a similar level of sensitivity to that observed with wild type AβPP (Fig. 1A, B). BMS299897 showed a similar profile of inhibition to DAPT and

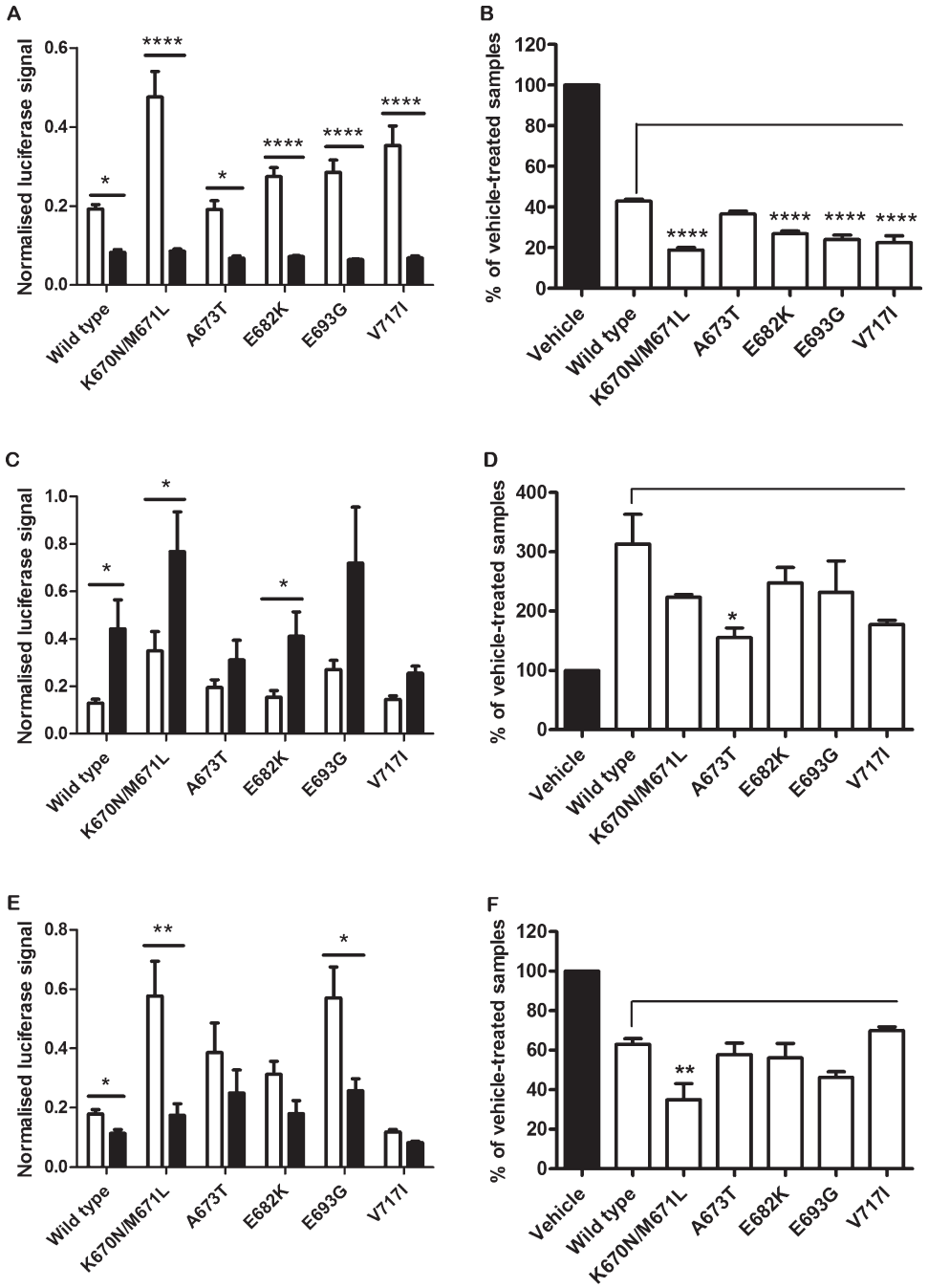

Fig. 1. AβPP GAL4 assay sensitivity to α-, β-, and γ-secretase inhibition. AβPP-GAL4 driven luciferase expression in the presence of the γ-secretase inhibitor DAPT (A, B); the α-secretase inhibitor TAPI-1 (C, D) or the β-secretase inhibitor β-IV (E, F). Primary cultured cortical neurons at 5-7 DIV were treated with vehicle (A, C, and E; white bars), 10 μM DAPT (A, black bars), 50 μM TAPI-1 (C, black bars), or 10 μM β-IV (E, black bars) for 30 min and then co-transfected with AβPP695-GAL4 wild type or AβPP-GAL4 mutants, pFR-Luc Firefly luciferase and phRL-TK. Dual-Glo luciferase activity assays were performed 24 h after transfection for quantification of Firefly and Renilla luciferase expression. Data presented in A, C, E, is Firefly luciferase reporter activity normalized to the constitutive Renilla activity. Each column is the mean ± SEM of 6–8 separate transfections prepared from at least 2 independent cultures ($^{*}p < 0.05$; $^{**}p < 0.01$; $^{***}p < 0.001$; $p < 0.0001$, $n = 6$-8; by two-way ANOVA with Bonferroni *post hoc* test) vehicle versus DAPT (A), vehicle versus TAPI-1 (C) vehicle versus β-IV (E). B, D, F) Present transformed data as a % of the paired vehicle control (shown as 100% black bar) to enable direct comparisons of the secretase sensitivity to be made between wild type AβPP and AβPP mutants following treatment with DAPT (B), TAPI-1 (D), and β-IV (F); ($^{*}p < 0.05$; $^{**}p < 0.01$; $^{***}p < 0.001$; $^{****}p < 0.0001$, $n = 6$–8; by one-way ANOVA with Bonferroni *post hoc* test).

the K670N/M671L mutation was significantly more sensitive to the inhibitor than wild type AβPP-GAL4 (Supplementary Fig. 1). Collectively, this data confirms the assay as an effective γ-secretase reporter and additionally highlights some differences in sensitivity to γ secretase inhibitors between AβPP mutants.

Although the underlying principle of our assay is to report γ-secretase processing, the dependency on α- and β-secretase is much more difficult to predict as the AICD can theoretically be generated by either α- or β-secretase processing. AβPP processing is tightly regulated in primary neurons with some inverse coupling observed between α- and β-secretase-mediated cleavage events [34] and the potential roles played by α- and β-secretase in AICD generation is a little controversial [35–38]. To first assess potential sensitivity to α-secretase-mediated processing two structurally distinct broad spectrum ADAM metalloprotease inhibitors, TAPI-1 and Batimastat were tested (Fig. 1C, D; Supplementary Fig. 2). Cortical neurons were treated with either TAPI-1 (50 μM) or Batimastat (50 μM) 30 min prior to transfection with the respective AβPP-GAL4 and reporter constructs and luciferase expression measured 24 h later. TAPI-1 treatment resulted in a 240% increase in luciferase expression resulting from processing of wild type AβPP-GAL4 and there was a similar level of potentiation with the K670N/M671L (220%) and E693G (265%) mutants (Fig. 1C). AβPP-GAL4 A673T was not significantly potentiated by TAPI-1 and was the least affected of all the mutants tested (Fig. 1D). Batimastat treatment also strongly increased AβPP-GAL4 driven luciferase expression with all AβPP-GAL4 reporter constructs equally affected (∼3-fold stimulation) (Supplementary Fig. 2A). This increase in luciferase expression most likely results from enhanced substrate (C89/C99) availability for β-secretase as we have previously reported [15]. To confirm this, we treated neurons with TAPI-1 and then assessed the levels of β-CTFs by immunoblotting. As predicted, chronic exposure to TAPI-1 imbalanced normal C83/C89/C99 distribution leading to increased levels of β-CTFs (Supplementary Fig. 2B). TAPI is a broad spectrum non-selective inhibitor and the constitutive α-secretase in neurons is most likely ADAM10 [39], so the effect of a more selective ADAM10 inhibitor (GI 254023X) was also investigated. Exposure to GI 254023X also showed a trend toward enhanced AβPP-GAL4 driven luciferase expression although less dramatically than that seen with Batimastat and TAPI-1 (Supplementary Fig. 2C). Collectively, this demonstrates that chronic and broad inhibition of α-secretase does not inhibit constitutive AICD production in neurons. To next assess sensitivity to β-secretase-mediated processing, neurons were treated with β-secretase inhibitor IV (10 μM) 30 min prior to transfection with the respective AβPP-GAL4 and reporter constructs, and luciferase expression measured 24 h later. β-IV inhibitor treatment resulted in a 36% decrease in luciferase expression resulting from processing of wild type AβPP-GAL4, 55% inhibition resulting from processing of the E693G mutant and a much more substantial 70% inhibition resulting from processing of the K670N/M671L mutant (Fig. 1E, F). None of the other AβPP-GAL4 constructs, including A673T, were significantly affected by the β-secretase inhibitor although there were clear trends toward lower luciferase expression with all mutants (Fig. 1E, F). We did expect to see a greater level of sensitivity of E682K to β-secretase inhibition but this did not reach significance mainly due a high level of variance with this construct. Collectively, this data indicates that in neurons the AβPP-GAL4 assay: reports βγ-secretase activity; is reciprocally modulated by β- and α-secretase inhibitors; is sensitive to mutations that increase β-secretase processing and Aβ production; and is sensitive to mutations which reduce β-secretase processing.

AβPP-GAL4 driven luciferase expression is enhanced by co-transfection with Fe65

AICD is a labile fragment, stabilized by association with Fe65 and forms a transcriptionally active complex with Fe65 and Tip60 [10, 40]. To determine if Fe65 enhanced luciferase expression in our assay neurons were co-transfected with Fe65 to assess the impact on AβPP-GAL4 driven luciferase expression. Fe65 enhanced luciferase gene expression driven by γ-secretase processing of either the AβPP-GAL4 wild type, K670N/M671L or A673T mutants. The greatest level of potentiation was observed with AβPP-GAL4 A673T and in the presence of Fe65 luciferase levels were the same as that following processing of AβPP-GAL4 K670N/M671L (Fig. 2A). To next determine if these potentiated signals resulted from β-secretase processing of AβPP the effect of β-IV and a structurally distinct β-secretase inhibitor AZD3839 were tested. AZD3839 and β-IV caused concentration-dependent inhibition of luciferase expression following processing of AβPP-GAL4 K670N/M671L (Fig. 2B) or

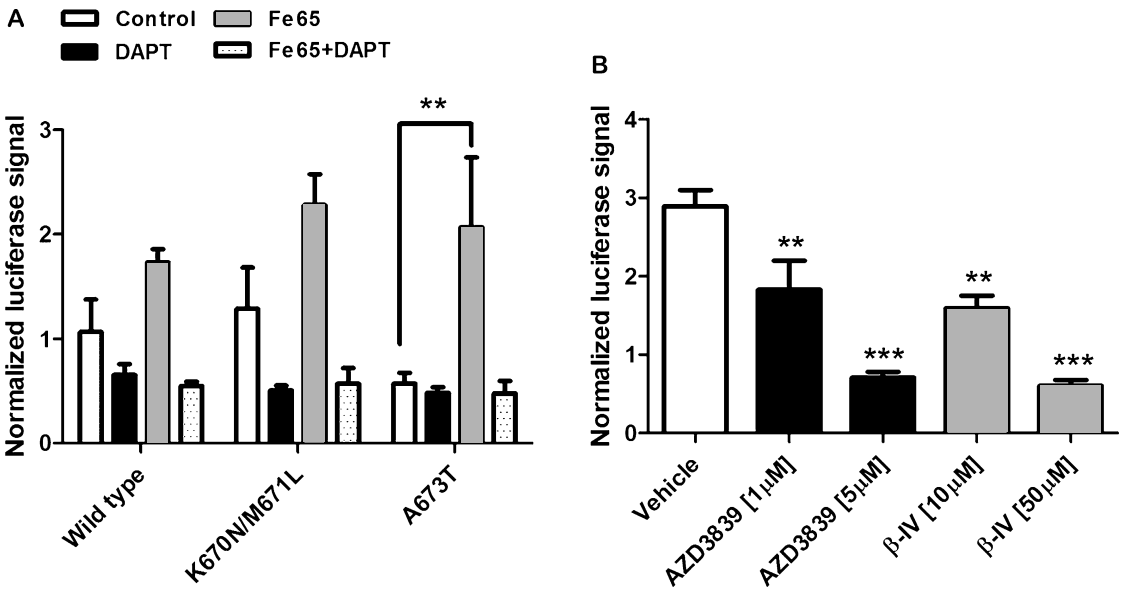

Fig. 2. Fe65 enhances β-secretase dependent AβPP-GAL4 driven luciferase expression. A) Primary cultured cortical neurons at 5–7 DIV were treated with vehicle (white bars & grey bars) or 10 μM DAPT (black bars & checked bars) for 30 min and then co-transfected with pFR-Luc Firefly luciferase and phRL-TK with, AβPP695-GAL4 wild type, AβPP-GAL4 K670N/M671L, or AβPP-GAL4 A673T either with (grey bars & checked bars) or without (white bars & black bars) Fe65. Dual-Glo luciferase activity assays were performed 24 h after transfection for quantification of Firefly and Renilla luciferase expression. Data presented is Firefly luciferase reporter activity normalized to the constitutive Renilla activity. Each column is the mean ± SEM of 4 separate transfections showing potentiation of the luciferase signal from APP-GAL4 A673T in the presence of Fe65 ($^{**}p < 0.01$; $n = 4$; by two-way ANOVA with Bonferroni *post hoc* test). B) Primary cultured cortical neurons at 5–7 DIV were treated with vehicle (white bar), AZD3839 (black bars, 1 μM or 5 μM) or β-IV (grey bars, 10 or 50 μM) for 30 min and then co-transfected with AβPP695-GAL4 K670N/M671L, Fe65, pFR-Luc Firefly luciferase, and phRL-TK Dual-Glo luciferase activity assays were performed 24 h after transfection for quantification of Firefly and Renilla luciferase expression. Data presented is Firefly luciferase reporter activity normalized to the constitutive Renilla activity. Each column is the mean ± SEM of 4 separate transfections showing β-secretase sensitivity compared with vehicle control ($^{**}p < 0.01$; $^{***}p < 0.001$; $n = 4$; by one-way ANOVA with Dunnett's Multiple Comparison Test).

AβPP-GAL4 wild type (not shown). This demonstrated that the Fe65-stabilized signal likely resulted primarily from β-secretase processing further validating the assay as a readout of amyloidogenic processing and consistent with AICD production as a β-secretase mediated process. Furthermore, in order to fully delineate differences in processing between AβPP mutants, the assay is best undertaken without co-expression of Fe65 which masks differences in processing likely by stabilizing the product.

Expression and processing of AβPP-GAL4 FAD mutations induces slowly developing neuronal damage

To be able to monitor AβPP processing in individual identifiable neurons the AβPP-GAL4 assay was adapted to report via a UAS-GFP system (Fig. 3A, B). To first confirm that GFP expression resulted from AβPP-GAL4-mediated secretase processing, the effects of TAPI-1, β-IV, and DAPT were tested and GFP positive cells counted. The number of cells expressing detectable GFP resulting from AβPP-GAL4 wild type processing was reduced by ∼85% by DAPT, reduced by ∼30% by β-IV, and increased by ∼50% by TAPI-1 (Fig. 3B), which was broadly in line with the pattern of regulation found with the luciferase reporter. The aim was to utilize this approach to probe for cellular changes lying downstream of AβPP processing that might mediate neuronal damage so a general morphological assessment of neuronal integrity was first made to define an appropriate time window for investigating responses occurring in advance of cell death. Neurons transfected with wild type, FAD, or protective AβPP-GAL4 constructs showed robust GFP expression within the cell soma, proximal axonal area, and neurites 24 h after transfection without obvious evidence of cell damage. However, by 96 h, neurons expressing AβPP-GAL4 FAD mutants showed swollen cell soma and damaged neurites (Fig. 3A, compare 24 h to 96 h). This was much less evident

with the AβPP-GAL4 wild type and there was no clear sign of damage in neurons expressing AβPP-GAL4 A673T (Fig. 3A). On this basis, we opted to use 24 h as the time-point for identifying signaling alterations resulting directly from the products of AβPP processing avoiding the potentially confounding effects caused by the release of secondary factors following cell damage at later stages.

Expression and processing of the AβPP-GAL4 K670N/M671L mutation increases nuclear localization of Foxo3a and enhances Foxo-mediated transcription

Foxo3a is a transcription factor that belongs to the O class of Forkhead Box proteins and may play a role in the regulation of neuronal apoptosis and autophagy in AD [28]. Furthermore, AβPP has been shown to modulate FoxO-mediated cell death through AICD, which acts as a transcriptional co-activator of FoxO [17]. We therefore wished to determine if AβPP processing coupled to the activation of Foxo3a in primary neurons. To first establish Foxo3a expression and basic susceptibility to dysregulated signaling in our model, neurons were treated with the PI3-kinase inhibitor wortmannin which allows Foxo3a to accumulate in the nucleus to drive transcription. Foxo3a localization was then determined by immunofluorescence. Under basal conditions, Foxo3a was distributed very diffusely throughout the cytoplasm and was excluded from the nucleus (Fig. 4A, upper panel). Exposure to wortmannin dramatically altered the staining profile with a strong co-localization of Foxo3a with DAPI positive nuclei now evident (Fig. 4A, lower panel). In order to determine if this redistribution of Foxo3a from cytoplasm to nucleus influenced its transcriptional activity we utilized a FoxO3a response element (FRE) luciferase reporter [32]. Exposure to wortmannin caused a modest but highly significant increase in FRE-mediated luciferase expression (Fig. 4B) consistent with enhanced Foxo3a mediated transcription following Foxo3a redistribution to the nucleus.

Next to assess whether AβPP processing impacted on Foxo3a, neurons were transfected with AβPP-GAL4 K670N/M671L and the UAS-GFP reporter and Foxo3a localization determined by immunofluorescence. The AβPP-GAL4 K670N/M671L mutant was utilized for these experiments as we hypothesized it should give us the clearest signal-to-noise outcome based on the earlier luciferase data. Foxo3a was clearly excluded from the nucleus of healthy non-transfected neurons (Fig. 4C, white arrows) but in neighboring transfected cells that were expressing and processing AβPP-GAL4 K670N/M671L, as determined by UAS-driven GFP expression, Foxo3a showed prominent nuclear staining and overlap with DAPI positive nuclei (Fig. 4C, Merge). Redistribution of Foxo3a in AβPP-GAL4 K670N/M671L expressing neurons resulted in enhanced FRE-mediated luciferase expression compared with neurons expressing AβPP-GAL4 wild type (Fig. 4D) suggesting a transcriptional gain of function associated with the K670N/M671L mutation. To determine if enhanced FRE-mediated luciferase expression resulted from secretase processing of AβPP-GAL4 K670N/M671L, neurons were treated with secretase inhibitors. There was a modest but clear trend towards reduced FRE-mediated luciferase expression in the presence of either DAPT (γ-secretase inhibitor) or β-IV (β-secretase inhibitor) but no inhibition in the presence of TAPI-1 (α-secretase inhibitor) (Fig. 4E). Collectively, this suggested that FRE-mediated transcription was downstream of amyloidogenic AβPP processing.

AICD has been proposed to physically associate with Foxo3a in the cytoplasm [17] and may co-translocate into the nucleus to drive an apoptotic transcriptional program. Thus, it was possible that our observed accumulation of Foxo3a in the nucleus of cells processing AβPP-GAL4 and the subsequent increase in transcription, resulted directly from production of the AICD. To address this, we transfected neurons with a GFP tagged AICD and then assessed the distribution of Foxo3a. AICD was expressed strongly throughout the neuronal cell soma and neurites but did not clearly stimulate nuclear accumulation of Foxo3a (Fig. 5A). In fact, we only observed clear nuclear Foxo3a in 3 out of 90 individual AICD-GFP transfected neurons across 3 coverslips. Despite, the lack of a strong visible translocation of Foxo3a there was an increase in FRE-luc activity in neurons transfected with AICD-GFP in comparison to neurons transfected with a UAS-GFP control plasmid (Fig. 5B), suggesting an increase in Foxo3a transcriptional activity directly downstream of AICD (Fig. 5B).

Processing of AβPP-GAL4 induces loss of pAkt at discrete locations

The PI3K/Akt signaling axis is strongly implicated in mediating neuronal responses to Aβ such as autophagy, mitophagy, plasticity and apoptosis

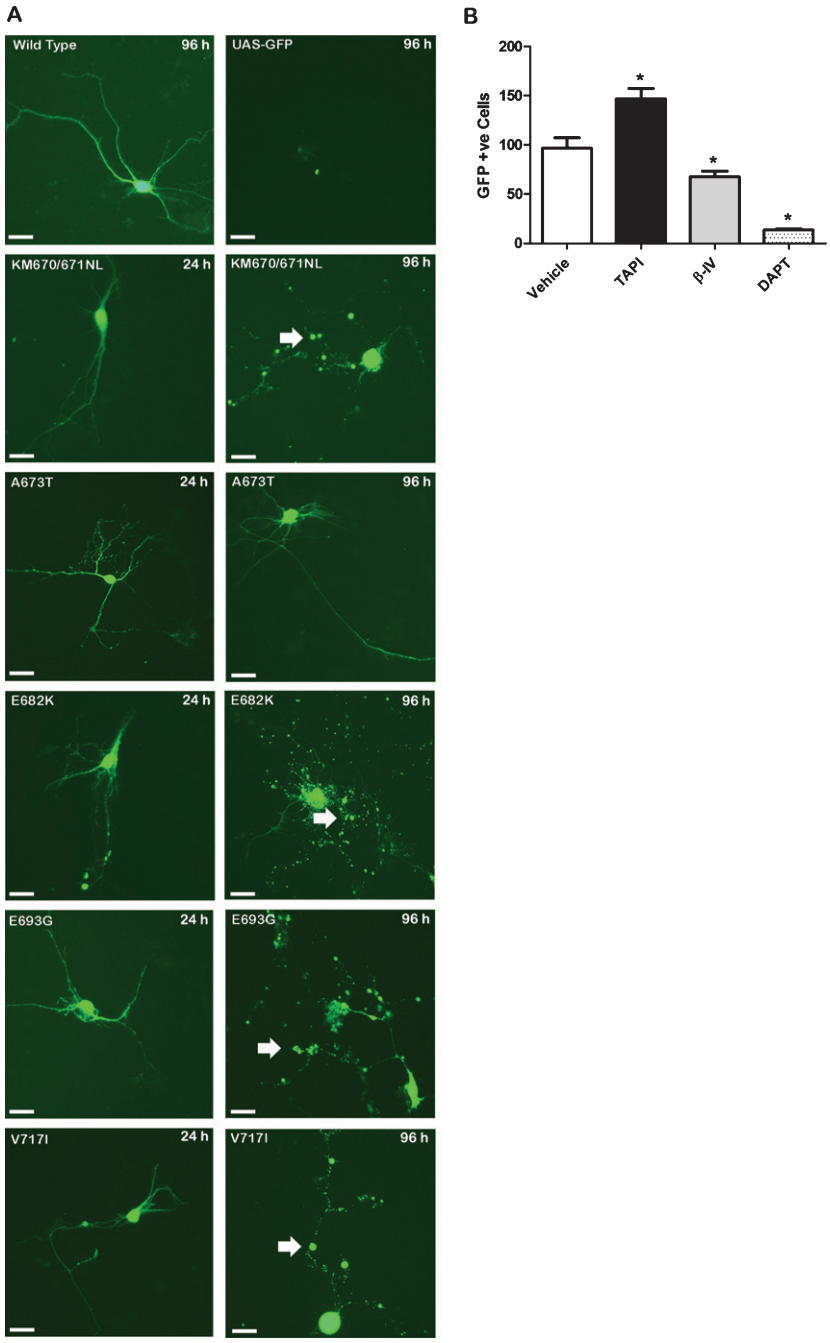

Fig. 3. AβPP-GAL4 driven GFP expression to visualize onset and development of neurotoxicity downstream of AβPP processing. A) Primary cultured cortical neurons at 5–7 DIV were transfected with, or without, AβPP695-GAL4 wild type or AβPP-GAL4 mutants and a UAS-GFP reporter and imaged for fluorescence at 24 h and 96 h post-transfection. Green fluorescence indicates transfected neurons expressing *and* processing AβPP-GAL4. At 24 h post transfection fluorescence was detectable in the cell soma and neurites of all AβPP-GAL4 mutants with no overt signs of cell damage. At 96 h, there were clear signs of damage to neurites in cells expressing and processing AβPP-GAL4 K670N/M671L, AβPP-GAL4 E682K, AβPP-GAL4 E693G, and AβPP-GAL4 V717L (white arrows) but less damage was detectable in neurons expressing AβPPA673T. No significant cellular fluorescence was observed in neurons transfected with UAS-GFP alone (UAS-GFP, 96 h). White scale bar (20 μm). B) Quantification of GFP positive cells in neurons following 30 min pre-treatment with TAPI-1 (50 μM; black bar), β-IV (10 μM; grey bar), DAPT (10 μM; speckled bar), or vehicle control (white bar) and then 24 h co-transfection with AβPP-GAL4 wild type and UAS-GFP. Each column are cell counts obtained from three coverslips from independently transfected neurons showing secretase sensitivity compared with vehicle control ($p < 0.05$; $n = 3$; by two tailed unpaired *t*-test).

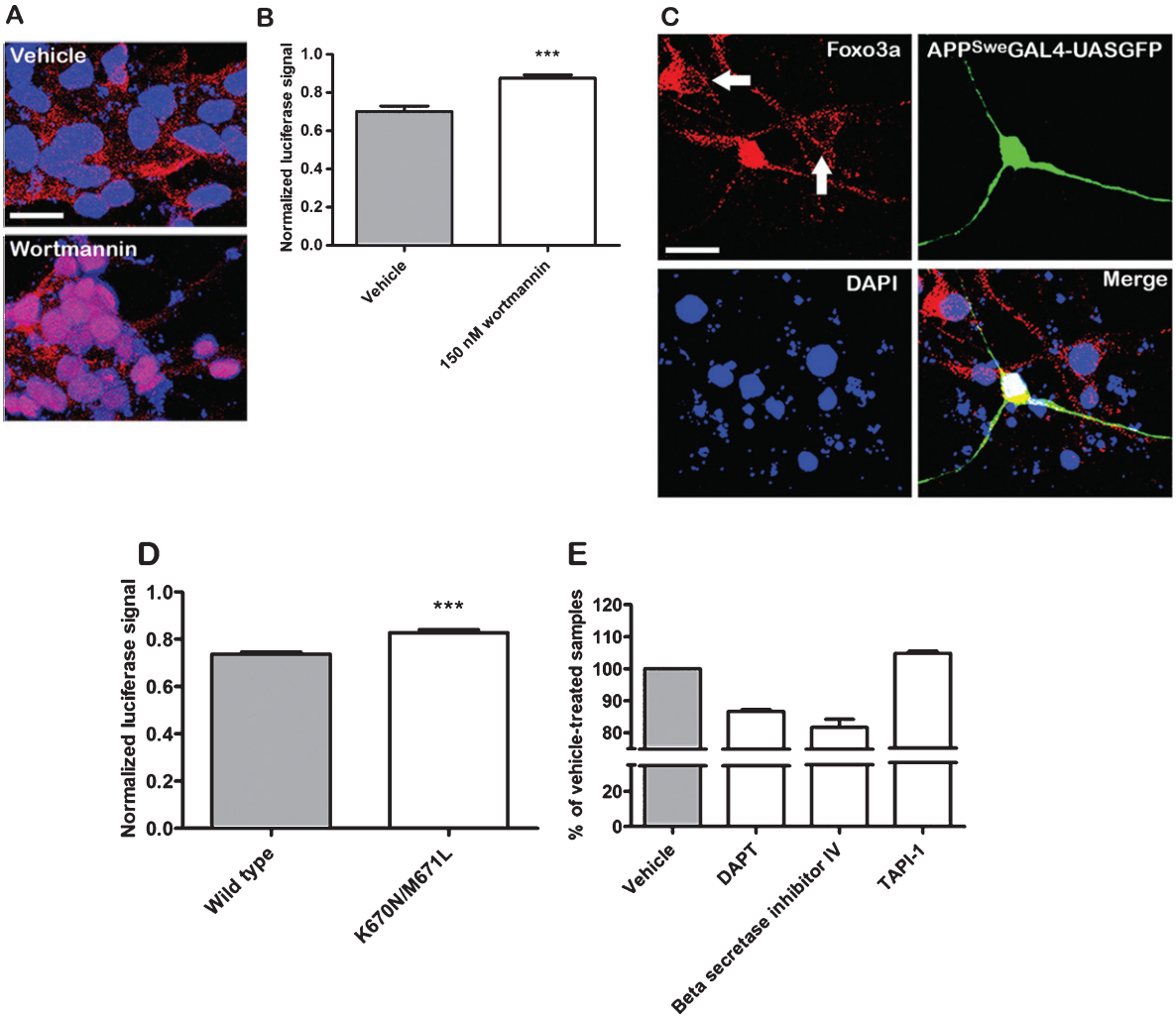

Fig. 4. AβPP-GAL4 processing increases nuclear accumulation and transcriptional activity of Foxo3a. A) Primary mouse cortical neurons at 7 DIV were treated with either vehicle or wortmannin (150 nM) for 2 h and the subcellular distribution of Foxo3a (red) determined by immunofluorescence. Nuclei were counterstained with DAPI (blue). Under vehicle conditions Foxo3a staining was very diffusely distributed, wortmannin treatment strongly increased the levels of nuclear Foxo3a (Scale bar = 20 μm). B) The effect of wortmannin treatment on the transcriptional activity of Foxo was determined using a FRE-Luc reporter construct. Neurons (5–7 DIV) were co-transfected with FRE-Luc and phRL-TK for 48 h and treated with 150 nM wortmannin, 2 h prior to being assayed for luciferase expression. Data presented is Firefly luciferase reporter activity normalized to the constitutive Renilla activity, following vehicle (grey bar) and wortmannin (white bar) treatment. Wortmannin increased Foxo driven luciferase expression compared with vehicle. (***$p < 0.001$; $n = 8$, by unpaired two tailed t-test). C) The effect of AβPP-GAL4 K670N/M671L (APP^{Swe}) expression and processing on Foxo3a distribution. Primary cultured cortical neurons at 6 DIV were co-transfected with UAS-GFP and AβPP-GAL4 K670N/M671L (APP^{Swe}) and fixed 48 h later for immunofluorescence staining with anti-Foxo3a (red), anti-GFP (green) and DAPI (blue). Merged image to illustrate localization of Foxo3a in the nucleus of neurons expressing and processing APP-GAL4 ^{Swe}. Note diffuse non-nuclear distribution of Foxo3a in neighboring non-transfected cells (white arrows). White scale bar (20 μm). D) Neurons (5–7 DIV) were co-transfected with FRE-Luc, phRL-TK and either AβPP-GAL4 wild type (grey bar) or AβPP-GAL4 K670N/M671L (white bar) and Dual-Glo luciferase activity assays were performed after 48 h for quantification of Firefly and Renilla luciferase expression. Data presented is Firefly luciferase reporter activity normalized to the constitutive Renilla activity. Each column is the mean ± SEM of 10 separate transfections from at least 2 independent cultures showing potentiation of the luciferase signal from AβPP-GAL4 K670N/M671L expressing neurons compared with AβPP-GAL4 wild type (***$p < 0.001$; $n = 10$; by unpaired t-test). E) Neurons (5-7DIV) were co-transfected with FRE-Luc, phRL-TK and AβPP-GAL4 K670N/M671L and treated with either vehicle (grey bar), DAPT (10 μM), β-IV (10 μM), or TAPI-1 (50 μM) and Dual-Glo luciferase activity assays were performed for quantification of Firefly and Renilla luciferase expression 48 h later. Data presented is Firefly luciferase reporter activity normalized to the constitutive Renilla activity. Each column is the mean ± SEM of 8 separate transfections from at least 2 independent cultures.

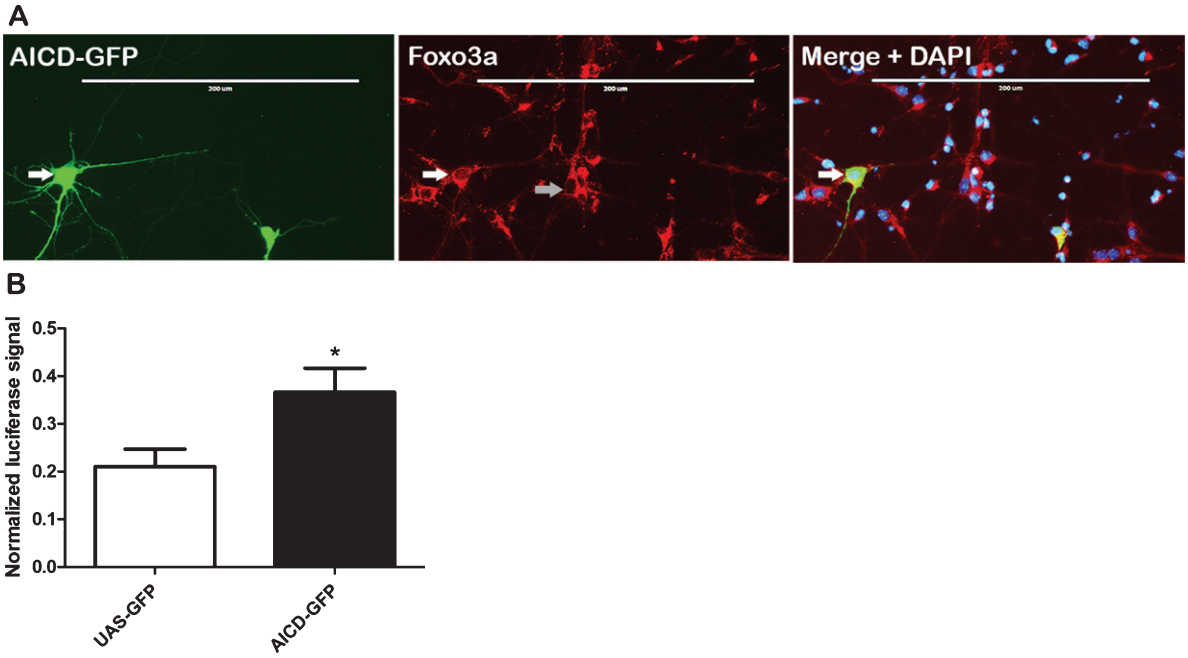

Fig. 5. Overexpression of AICD-GFP does not drive Foxo3a translocation but enhances Foxo transcription. A) Primary cortical neurons at 6DIV were transfected with pEGFP-n1-AICD (AICD-GFP, green) overnight and the distribution of Foxo3a (red) determined by immunofluorescence. Nuclei were counterstained with DAPI (blue). Note general pattern of diffuse non-nuclear distribution of Foxo3a in both transfected (white arrows) and neighboring non-transfected cells (grey arrow central panel). White scale bar (200 μm). B) Neurons (6DIV) were co-transfected with FRE-Luc, phRL-TK and either UAS-GFP (white bar) or pEGFP-n1-AICD (AICD-GFP, black bar) and Dual-Glo luciferase activity assays were performed after 24 h for quantification of Firefly and Renilla luciferase expression. Data presented is Firefly luciferase reporter activity normalized to the constitutive Renilla activity. Each column is the mean ± SEM of 6 separate transfections showing potentiation of the luciferase signal from AICD-GFP expressing neurons compared with the UAS-GFP control ($^{*}p < 0.05$; $n = 6$; by unpaired *t*-test).

and we have previously reported a marked loss of pAkt in AβPP transgenic mouse brain in the absence of neuronal cell death [25]. Loss of Akt-mediated phosphorylation on Ser^{253} promotes Foxo3a nuclear localization and increases the transcription of pro-apoptotic genes [24]. We therefore wished to determine if β-secretase mediated AβPP-GAL4 processing impaired pAkt. Basal levels of pAkt were high in all cells, consistent with previous observations, but in neurons expressing AβPP-GAL4, and most notably the K670N/M671L mutation, there was evidence of a loss of pAkt in discrete parts of the cell (Fig. 6A, B). Reduced pAkt was most evident in neuritic locations lying close to the cell soma and in the proximal axon (Fig. 6A, B) suggesting these regions might be most vulnerable to the products of βγ-secretase processing. There was no evidence of loss of pAkt in immediate neighboring non-transfected cells indicating that this signaling deficit results from cellular expression and processing of AβPP-GAL4 and suggests that this might not be mediated by a secreted factor. Although we have not demonstrated a direct causal relationship, these observations do suggest that Foxo3a translocation correlates with a loss of Akt phosphorylation, which would be consistent with a loss of regulation of Foxo3a by Akt.

DISCUSSION

We have adapted and characterized an AβPP-GAL4 luciferase and GFP gene reporter assay in primary mouse cortical neurons as a model system for testing physiological, pathological, genetic and environmental influences on AβPP processing, for probing cellular responses lying downstream of AβPP processing and as a platform for screening secretase inhibitors. This represents a complete system for studying the influence of AβPP processing on synaptic function and dysfunction incorporating all the elements and products of the AβPP processing pathways which are lacking in approaches applying recombinant Aβ to cells. Although the development of iPS cell systems ultimately has the potential to

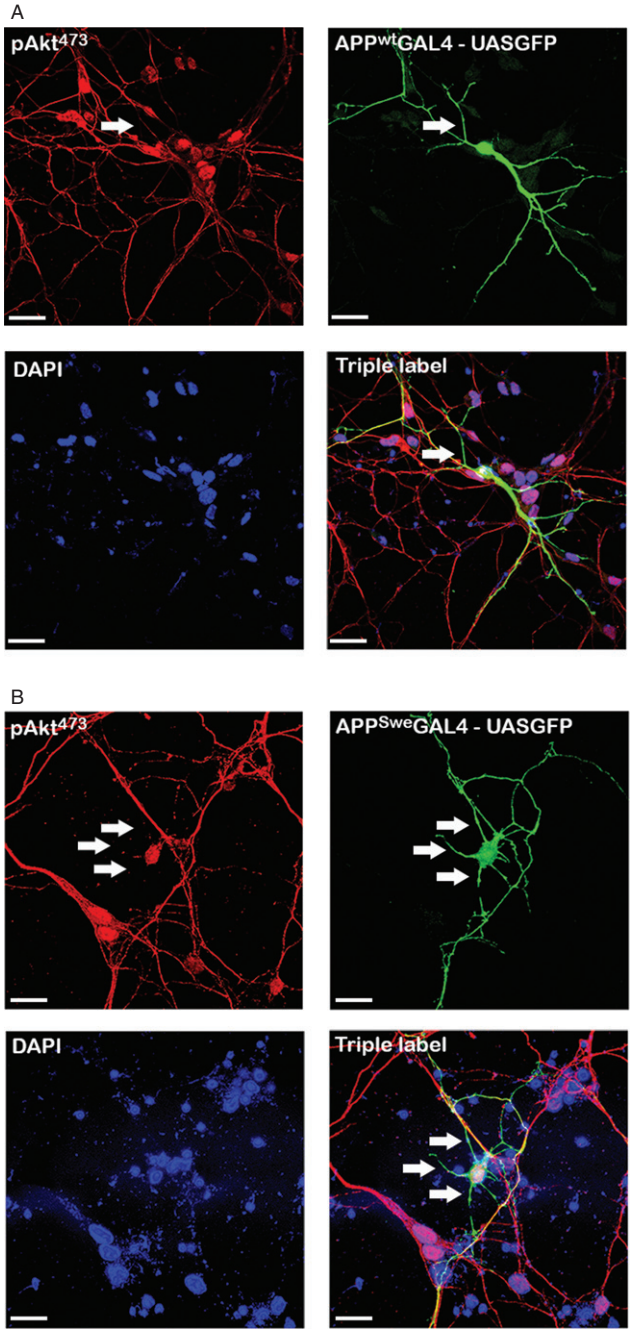

Fig. 6. AβPP-GAL4 processing induces a loss of Akt phosphorylation at discrete sites. Primary cultured cortical neurons at 5–8 DIV were co-transfected with UAS-GFP and either AβPP-GAL4 wild type (A) or AβPP-GAL4 K670N/M671L (APP^{Swe}) (B) and fixed 24 h later for immunofluorescence staining with anti-pAkt473 (red), anti-GFP (green) and DAPI (blue). Triple label is the merged image to illustrate pAkt deficits (white arrows) observed at discrete neuronal locations in cells expressing and processing AβPP-GAL4. Note the high levels of $pAkt^{473}$ throughout the cell soma, neurites and axons of neighboring non-transfected cells. White scale bar (20 μm).

offer similar outcomes, rodent neurons have very well characterized synaptic physiology and are simple to maintain and differentiate so this approach has valuable utility.

When expressed in neurons the AβPP-GAL4 reporter assay was sensitive to γ-secretase inhibition as expected, and preferentially reported βγ-secretase processing over αγ-secretase processing. β-secretase

inhibitors reduced luciferase expression whereas broad-spectrum α-secretase inhibitors potentiated luciferase expression. This reciprocal sensitivity to secretase inhibition was consistent with ADAM metalloproteases and BACE1 competing for AβPP as a substrate, such that their cleavages are inversely coupled [34]. This mechanism provides a possible explanation for the association between late-onset AD-associated mutations in ADAM10 and enhanced Aβ levels [41]. Others, however, have only observed unidirectional coupling with ADAM10 inhibition not influencing BACE processing of endogenous mouse AβPP [34], so it appears that the precise cellular context and/or presence of human AβPP695 could be critical determinants for detecting this reciprocal relationship. In our hands, inhibition of α-secretase processing of AβPP at the plasma membrane by TAPI-1 increased the levels of the AβPP carboxyl-terminal fragment (β-CTF) potentially providing more substrate availability to BACE1 within the trans-Golgi network. Amyloidogenic processing of AβPP is associated with the appearance of mature differentiated cortical phenotypes in human iPS cells [42], and we observed similar β-secretase favored processing of human AβPP-GAL4 in mouse cortical neurons differentiated from E15 embryos, giving us confidence in the basic utility of a system expressing human AβPP695 on a rodent background. Significantly, mutations in AβPP, such as the K670N/M671L mutation which enhances BACE processing, showed the highest levels of AβPP-GAL4 mediated gene expression and greatest sensitivity to β-secretase inhibition compared with wild type AβPP and other AβPP mutants. The protective A673T mutation which has been shown to reduce BACE processing coupled weakly to AβPP-GAL4 mediated gene expression and showed least sensitivity to β-secretase inhibition and no clear signal potentiation in the presence of the α-secretase inhibitor TAPI-1. This is in agreement with findings that the A673T substitution makes AβPP a less favorable substrate for cleavage by BACE1 [43]. Collectively, this demonstrated that the assay is sensitive to bi-directional genetic influences on β-secretase-mediated AβPP processing. AβPP-GAL4-mediated luciferase expression was strongly potentiated upon co-transfection of neurons with Fe65, even with the A673T mutation, likely due to a stabilizing and accumulating effect on the AICD leading to increased expression of the reporter [10, 40]. This is important as it shows that in order to fully delineate differences in processing between AβPP mutants, the assay is best undertaken without co-expression of Fe65 which masks subtle differences in processing likely by stabilizing the product. Furthermore, the inherent sensitivity of the assay to β-secretase inhibition, either in the presence or absence of Fe65, is in agreement with functional AICD appearing to be preferentially synthesized via β-secretase action on AβPP695 in neurons [35, 38, 44].

To test the utility of our system for probing early neuronal responses to amyloidogenic AβPP processing at the single cell level, we coupled the reporter to a GFP readout and confirmed that GFP expression was also dependent on γ-secretase and, albeit to a lesser extent, β-secretase-mediated processing. Prolonged expression of all of the AβPP695 constructs ultimately initiated some degree of cell damage, so we chose 24 h post-transfection to investigate signaling changes lying downstream of AβPP processing and upstream of overt neurotoxicity. We adopted a deliberately biased strategy here focusing on Akt/PKB and Foxo3a as molecular targets, as we already had evidence of impaired Akt phosphorylation from previous AβPP transgenic mouse studies [25] and wished to determine if similar deficits could be detected *in vitro*. Processing of AβPP-GAL4, and most notably AβPP containing the K670N/M671L double mutation, caused loss of pAkt at very discrete neuritic locations. The molecular explanation for the reduction in pAkt was not clear but could have resulted either from impaired receptor input into the PI3K-Akt axis and/or upregulation of phosphatases. For example, Aβ binds to and internalizes AMPA receptors (AMPAR) following upregulation of the lipid kinase PTEN to mediate Aβ-induced synaptic depression [45] which could reduce basal AMPA and NMDA receptor signaling to pAkt [46, 47] at glutamatergic synapses. The caveat to this is that there was no obvious Akt deficit in neighboring non-transfected cells which could argue against a simple mechanism involving secreted Aβ and as such the mechanisms underlying aberrant neuronal Akt signaling need further investigation.

To determine if loss of pAkt triggered further cellular dysregulation, we investigated the activity of Foxo3a. Foxo3a is a transcription factor that belongs to the O class of Forkhead Box protein [48, 49] controlling expression of pro-apoptotic genes such as Fas ligand [24, 50] and Bim [51] and regulating caspase-mediated apoptosis [52]. Foxo3a has been

implicated in the development of protein pathology in neurodegenerative disease [26, 27] through apoptosis and autophagy [28, 52] and via the mediation of microglial responses to Aβ [53]. Moreover, in Drosophila and mammalian cells AβPP modulates FoxO-mediated cell death through AICD, which associates with FoxO in the cytoplasm then acts as a transcriptional co-activator [17]. Foxo3a activity is also regulated by a number of post-translational modifications and loss of phosphorylation by the pro-survival kinase Akt leads to its dissociation from the negative regulator 14-3-3 protein and promotes Foxo3a nuclear localization and transcriptional activity [24]. Consistent with this, we observed nuclear accumulation of Foxo3a in neurons expressing and processing AβPP-GAL4 which resulted in enhanced Foxo-mediated transcription in a secretase-sensitive manner. We could not demonstrate a strong direct relationship between AICD and Foxo3a translocation although it is possible that the GFP tag on AICD prevented its translocation into the nucleus. AICD overexpression did, however, modestly enhance Foxo-driven luciferase expression consistent with its proposed role as a transcriptional co-activator. Thus, it would appear that amyloidogenic AβPP processing couples to enhanced Foxo3a activity through production of the AICD and stimulates Foxo3a translocation following a loss of pAkt. Emerging evidence places Foxo3a as a possible molecular target in AD therapeutic development [28] and recent meta-analysis of direct FOXO targets has highlighted AD–presenilin pathway genes [54] so this assay could have potential utility in identifying inhibitors and modulators of these pathways in neurons.

Conclusion

We have adapted an AβPP-GAL4 reporter construct, introducing familial disease associated mutations into the AβPP695 sequence and coupling it to both luciferase and GFP reporters to monitor AβPP processing in primary mouse cortical neurons. This acts as a powerful model system for testing physiological, pathological, genetic, and environmental influences on AβPP processing, for screening secretase modulators and for probing cellular responses lying downstream of AβPP processing. Basic utility is demonstrated by showing upregulation of Foxo3a nuclear translocation and activity in neurons linked to amyloidogenic AβPP processing.

ACKNOWLEDGMENTS

This work was supported by a project grant to RJW from BRACE (Funding Research into Alzheimer's Disease).

Authors' disclosures available online (https://www.j-alz.com/manuscript-disclosures/17-0393r2).

SUPPLEMENTARY MATERIAL

The supplementary material is available in the electronic version of this article: http://dx.doi.org/10.3233/JAD-170393.

REFERENCES

[1] Karran E, De Strooper B (2016) The amyloid cascade hypothesis: Are we poised for success or failure? *J Neurochem* **139**(Suppl 2), 237-252.

[2] Selkoe DJ, Hardy J (2016) The amyloid hypothesis of Alzheimer's disease at 25 years. *EMBO Mol Med* **8**, 595-608.

[3] De Strooper B, Karran E (2016) The cellular phase of Alzheimer's disease. *Cell* **164**, 603-615.

[4] Hussain I, Powell D, Howlett DR, Tew DG, Meek TD, Chapman C, Gloger IS, Murphy KE, Southan CD, Ryan DM, Smith TS, Simmons DL, Walsh FS, Dingwall C, Christie G (1999) Identification of a novel aspartic protease (Asp 2) as beta-secretase. *Mol Cell Neurosci* **14**, 419-427.

[5] Sinha S, Anderson JP, Barbour R, Basi GS, Caccavello R, Davis D, Doan M, Dovey HF, Frigon N, Hong J, Jacobson-Croak K, Jewett N, Keim P, Knops J, Lieberburg I, Power M, Tan H, Tatsuno G, Tung J, Schenk D, Seubert P, Suomensaari SM, Wang S, Walker D, Zhao J, McConlogue L, John V (1999) Purification and cloning of amyloid precursor protein beta-secretase from human brain. *Nature* **402**, 537-540.

[6] Vassar R, Bennett BD, Babu-Khan S, Kahn S, Mendiaz EA, Denis P, Teplow DB, Ross S, Amarante P, Loeloff R, Luo Y, Fisher S, Fuller J, Edenson S, Lile J, Jarosinski MA, Biere AL, Curran E, Burgess T, Louis JC, Collins F, Treanor J, Rogers G, Citron M (1999) Beta-secretase cleavage of Alzheimer's amyloid precursor protein by the transmembrane aspartic protease BACE. *Science* **286**, 735-741.

[7] Yan R, Bienkowski MJ, Shuck ME, Miao H, Tory MC, Pauley AM, Brashier JR, Stratman NC, Mathews WR, Buhl AE, Carter DB, Tomasselli AG, Parodi LA, Heinrikson RL, Gurney ME (1999) Membrane-anchored aspartyl protease with Alzheimer's disease beta-secretase activity. *Nature* **402**, 533-537.

[8] De Strooper B, Saftig P, Craessaerts K, Vanderstichele H, Guhde G, Annaert W, Von Figura K, Van Leuven F (1998) Deficiency of presenilin-1 inhibits the normal cleavage of amyloid precursor protein. *Nature* **391**, 387-390.

[9] Wolfe MS, Xia W, Ostaszewski BL, Diehl TS, Kimberly WT, Selkoe DJ (1999) Two transmembrane aspartates in presenilin-1 required for presenilin endoproteolysis and gamma-secretase activity. *Nature* **398**, 513-517.

[10] Cao X, Südhof TC (2001) A transcriptionally active complex of APP with Fe65 and histone acetyltransferase Tip60. *Science* **293**, 115-120.

[11] Lammich S, Kojro E, Postina R, Gilbert S, Pfeiffer R, Jasionowski M, Haass C, Fahrenholz F (1999) Constitutive and regulated alpha-secretase cleavage of Alzheimer's amyloid precursor protein by a disintegrin metalloprotease. *Proc Natl Acad Sci U S A* **96**, 3922-3927.

[12] Gianni D, Zambrano N, Bimonte M, Minopoli G, Mercken L, Talamo F, Scaloni A, Russo T (2003) Platelet-derived growth factor induces the beta-gamma-secretase-mediated cleavage of Alzheimer's amyloid precursor protein through a Src-Rac-dependent pathway. *J Biol Chem* **278**, 9290-9297.

[13] Bakshi P, Liao YF, Gao J, Ni J, Stein R, Yeh LA, Wolfe MS (2005) A high-throughput screen to identify inhibitors of amyloid beta-protein precursor processing. *J Biomol Screen* **10**, 1-12.

[14] Zhang C, Khandelwal PJ, Chakraborty R, Cuellar TL, Sarangi S, Patel SA, Cosentino CP, O'Connor M, Lee JC, Tanzi RE, Saunders AJ (2007) An AICD-based functional screen to identify APP metabolism regulators. *Mol Neurodegener* **2**, 15.

[15] Hoey SE, Williams RJ, Perkinton MS (2009) Synaptic NMDA receptor activation stimulates alpha-secretase amyloid precursor protein processing and inhibits amyloid-beta production. *J Neurosci* **29**, 4442-4460.

[16] Hoey SE, Buonocore F, Cox CJ, Hammond VJ, Perkinton MS, Williams RJ (2013) AMPA receptor activation promotes non-amyloidogenic amyloid precursor protein processing and suppresses neuronal amyloid-β production. *PLoS One* **8**, e78155.

[17] Wang X, Wang Z, Chen Y, Huang X, Hu Y, Zhang R, Ho MS, Xue L (2014) FoxO mediates APP-induced AICD-dependent cell death. *Cell Death Dis* **5**, e1233.

[18] De Jonghe C, Esselens C, Kumar-Singh S, Craessaerts K, Serneels S, Checler F, Annaert W, Van Broeckhoven C, De Strooper B (2001) Pathogenic APP mutations near the gamma-secretase cleavage site differentially affect Abeta secretion and APP C-terminal fragment stability. *Hum Mol Genet* **10**, 1665-1671.

[19] Nilsberth C, Westlind-Danielsson A, Eckman CB, Condron MM, Axelman K, Forsell C, Stenh C, Luthman J, Teplow DB, Younkin SG, Näslund J, Lannfelt L (2001) The 'Arctic' APP mutation (**E693G**) causes Alzheimer's disease by enhanced Abeta protofibril formation. *Nat Neurosci* **4**, 887-893.

[20] Mullan M, Crawford F, Axelman K, Houlden H, Lilius L, Winblad B, Lannfelt L (1992) A pathogenic mutation for probable Alzheimer's disease in the APP gene at the N-terminus of beta-amyloid. *Nat Genet* **1**, 345-347.

[21] Scheuner D, Eckman C, Jensen M, Song X, Citron M, Suzuki N, Bird TD, Hardy J, Hutton M, Kukull W, Larson E, Levy-Lahad E, Viitanen M, Peskind E, Poorkaj P, Schellenberg G, Tanzi R, Wasco W, Lannfelt L, Selkoe D, Younkin S (1996) Secreted amyloid beta-protein similar to that in the senile plaques of Alzheimer's disease is increased *in vivo* by the presenilin 1 and 2 and APP mutations linked to familial Alzheimer's disease. *Nat Med* **2**, 864-870.

[22] Zhou L, Brouwers N, Benilova I, Vandersteen A, Mercken M, Van Laere K, Van Damme P, Demedts D, Van Leuven F, Sleegers K, Broersen K, Van Broeckhoven C, Vandenberghe R, De Strooper B (2011) Amyloid precursor protein mutation E682K at the alternative β-secretase cleavage β'-site increases Aβ generation. *EMBO Mol Med* **3**, 291-302.

[23] Jonsson T, Atwal JK, Steinberg S, Snaedal J, Jonsson PV, Bjornsson S, Stefansson H, Sulem P, Gudbjartsson D, Maloney J, Hoyte K, Gustafson A, Liu Y, Lu Y, Bhangale T, Graham RR, Huttenlocher J, Bjornsdottir G, Andreassen OA, Jönsson EG, Palotie A, Behrens TW, Magnusson OT, Kong A, Thorsteinsdottir U, Watts RJ, Stefansson K (2012) A mutation in APP protects against Alzheimer's disease and age-related cognitive decline. *Nature* **488**, 96-99.

[24] Brunet A, Bonni A, Zigmond MJ, Lin MZ, Juo P, Hu LS, Anderson MJ, Arden KC, Blenis J, Greenberg ME (1999) Akt promotes cell survival by phosphorylating and inhibiting a Forkhead transcription factor. *Cell* **96**, 857-868.

[25] Abbott JJ, Howlett DR, Francis PT, Williams RJ (2008) Abeta(1-42) modulation of Akt phosphorylation via alpha7 nAChR and NMDA receptors. *Neurobiol Aging* **29**, 992-1001.

[26] Su B, Liu H, Wang X, Chen SG, Siedlak SL, Kondo E, Choi R, Takeda A, Castellani RJ, Perry G, Smith MA, Zhu X, Lee HG (2009) Ectopic localization of FOXO3a protein in Lewy bodies in Lewy body dementia and Parkinson's disease. *Mol Neurodegener* **4**, 32.

[27] Perez FP, Bose D, Maloney B, Nho K, Shah K, Lahiri DK (2014) Late-onset Alzheimer's disease, heating up and foxed by several proteins: Pathomolecular effects of the aging process. *J Alzheimers Dis* **40**, 1-17.

[28] Maiese K (2016) Forkhead transcription factors: New considerations for alzheimer's disease and dementia. *J Transl Sci* **2**, 241-247.

[29] Zhan H, Gong Z (2010) Delayed and restricted expression of UAS-regulated GFP gene in early transgenic zebrafish embryos by using the GAL4/UAS system. *Mar Biotechnol (NY)* **12**, 1-7.

[30] Currinn H, Guscott B, Balklava Z, Rothnie A, Wassmer T (2016) APP controls the formation of PI(3,5)P(2) vesicles through its binding of the PIKfyve complex. *Cell Mol Life Sci* **73**, 393-408.

[31] Guo S, Rena G, Cichy S, He X, Cohen P, Unterman T (1999) Phosphorylation of serine 256 by protein kinase B disrupts transactivation by FKHR and mediates effects of insulin on insulin-like growth factor-binding protein-1 promoter activity through a conserved insulin response sequence. *J Biol Chem* **274**, 17184-17192.

[32] Bahia PK, Pugh V, Hoyland K, Hensley V, Rattray M, Williams RJ (2012) Neuroprotective effects of phenolic antioxidant tBHQ associate with inhibition of FoxO3a nuclear translocation and activity. *J Neurochem* **123**, 182-191.

[33] Cox CJ, Choudhry F, Peacey E, Perkinton MS, Richardson JC, Howlett DR, Lichtenthaler SF, Francis PT, Williams RJ (2015) Dietary (-)-epicatechin as a potent inhibitor of βγ-secretase amyloid precursor protein processing. *Neurobiol Aging* **36**, 178-187.

[34] Colombo A, Wang H, Kuhn PH, Page R, Kremmer E, Dempsey PJ, Crawford HC, Lichtenthaler SF (2013) Constitutive α- and β-secretase cleavages of the amyloid precursor protein are partially coupled in neurons, but not in frequently used cell lines. *Neurobiol Dis* **49**, 137-147.

[35] Belyaev ND, Kellett KA, Beckett C, Makova NZ, Revett TJ, Nalivaeva NN, Hooper NM, Turner AJ (2010) The transcriptionally active amyloid precursor protein (APP) intracellular domain is preferentially produced from the 695 isoform of APP in a {beta}-secretase-dependent pathway. *J Biol Chem* **285**, 41443-41454.

[36] Sala Frigerio C, Fadeeva JV, Minogue AM, Citron M, Van Leuven F, Staufenbiel M, Paganetti P, Selkoe DJ, Walsh DM (2010) beta-Secretase cleavage is not required for generation of the intracellular C-terminal domain of the amyloid precursor family of proteins. *FEBS J* **277**, 1503-1518.

[37] Kim ML, Zhang B, Mills IP, Milla ME, Brunden KR, Lee VM (2008) Effects of TNFalpha-converting enzyme inhibition on amyloid beta production and APP processing in vitro and *in vivo*. *J Neurosci* **28**, 12052-12061.

[38] Flammang B, Pardossi-Piquard R, Sevalle J, Debayle D, Dabert-Gay AS, Thévenet A, Lauritzen I, Checler F (2012) Evidence that the amyloid-β protein precursor intracellular domain, AICD, derives from β-secretase-generated C-terminal fragment. *J Alzheimers Dis* **30**, 145-153.

[39] Kuhn PH, Wang H, Dislich B, Colombo A, Zeitschel U, Ellwart JW, Kremmer E, Rossner S, Lichtenthaler SF (2010) ADAM10 is the physiologically relevant, constitutive alpha-secretase of the amyloid precursor protein in primary neurons. *EMBO J* **29**, 3020-3032.

[40] Kimberly WT, Zheng JB, Guénette SY, Selkoe DJ (2001) The intracellular domain of the beta-amyloid precursor protein is stabilized by Fe65 and translocates to the nucleus in a notch-like manner. *J Biol Chem* **276**, 40288-40292.

[41] Kim M, Suh J, Romano D, Truong MH, Mullin K, Hooli B, Norton D, Tesco G, Elliott K, Wagner SL, Moir RD, Becker KD, Tanzi RE (2009) Potential late-onset Alzheimer's disease-associated mutations in the ADAM10 gene attenuate {alpha}-secretase activity. *Hum Mol Genet* **18**, 3987-3996.

[42] Bergström P, Agholme L, Nazir FH, Satir TM, Toombs J, Wellington H, Strandberg J, Bontell TO, Kvartsberg H, Holmström M, Boreström C, Simonsson S, Kunath T, Lindahl A, Blennow K, Hanse E, Portelius E, Wray S, Zetterberg H (2016) Amyloid precursor protein expression and processing are differentially regulated during cortical neuron differentiation. *Sci Rep* **6**, 29200.

[43] Maloney JA, Bainbridge T, Gustafson A, Zhang S, Kyauk R, Steiner P, van der Brug M, Liu Y, Ernst JA, Watts RJ, Atwal JK (2014) Molecular mechanisms of Alzheimer disease protection by the A673T allele of amyloid precursor protein. *J Biol Chem* **289**, 30990-31000.

[44] Goodger ZV, Rajendran L, Trutzel A, Kohli BM, Nitsch RM, Konietzko U (2009) Nuclear signaling by the APP intracellular domain occurs predominantly through the amyloidogenic processing pathway. *J Cell Sci* **122**, 3703-3714.

[45] Knafo S, Sánchez-Puelles C, Palomer E, Delgado I, Draffin JE, Mingo J, Wahle T, Kaleka K, Mou L, Pereda-Perez I, Klosi E, Faber EB, Chapman HM, Lozano-Montes L, Ortega-Molina A, Ordóñez-Gutiérrez L, Wandosell F, Viña J, Dotti CG, Hall RA, Pulido R, Gerges NZ, Chan AM, Spaller MR, Serrano M, Venero C, Esteban JA (2016) PTEN recruitment controls synaptic and cognitive function in Alzheimer's models. *Nat Neurosci* **19**, 443-453.

[46] Perkinton MS, Sihra TS, Williams RJ (1999) Ca(2+)-permeable AMPA receptors induce phosphorylation of cAMP response element-binding protein through a phosphatidylinositol 3-kinase-dependent stimulation of the mitogen-activated protein kinase signaling cascade in neurons. *J Neurosci* **19**, 5861-5874.

[47] Perkinton MS, Ip JK, Wood GL, Crossthwaite AJ, Williams RJ (2002) Phosphatidylinositol 3-kinase is a central mediator of NMDA receptor signalling to MAP kinase (Erk1/2), Akt/PKB and CREB in striatal neurones. *J Neurochem* **80**, 239-254.

[48] Kaestner KH, Knochel W, Martinez DE (2000) Unified nomenclature for the winged helix/forkhead transcription factors. *Genes Dev* **14**, 142-146.

[49] Barthel A, Schmoll D, Unterman TG (2005) FoxO proteins in insulin action and metabolism. *Trends Endocrinol Metab* **16**, 183-189.

[50] Barthélémy C1, Henderson CE, Pettmann B (2004) Foxo3a induces motoneuron death through the Fas pathway in cooperation with JNK. *BMC Neurosci* **5**, 48.

[51] Obexer P, Geiger K, Ambros PF, Meister B, Ausserlechner MJ (2007) FKHRL1-mediated expression of Noxa and Bim induces apoptosis via the mitochondria in neuroblastoma cells. *Cell Death Differ* **14**, 534-547.

[52] Maiese K, Chong ZZ, Shang YC (2007) "Sly as a FOXO": New paths with Forkhead signaling in the brain. *Curr Neurovasc Res* **4**, 295-302.

[53] Shang YC, Chong ZZ, Hou J, Maiese K (2009) The forkhead transcription factor FOXO3a controls microglial inflammatory activation and eventual apoptotic injury through caspase 3. *Curr Neurovasc Res* **6**, 20-31.

[54] Webb AE, Kundaje A, Brunet A (2016) Characterization of the direct targets of FOXO transcription factors throughout evolution. *Aging Cell* **15**, 673-685.